BIOCHEMISTRY
including biophysical chemistry & molecular biology
Article

*Biochemistry* **2010,** *49,* 10543–10552 10543
DOI: 10.1021/bi101398s

# DNA Binding Characteristics of Mithramycin and Chromomycin Analogues Obtained by Combinatorial Biosynthesis†

Francisca Barceló,‡ Miguel Ortiz-Lombardía,§ Miquel Martorell,‡ Miquel Oliver,‡ Carmen Méndez,∥ José A. Salas,∥ and José Portugal*,⊥

‡*Departament de Biologia Fundamental i Ciencies de la Salut, Universitat de les Illes Balears, Palma de Mallorca, Spain,* §*Architecture et Fonction des Macromolécules Biologiques (UMR6098), CNRS, Universités d'Aix-Marseille I & II, Marseille, France,* ∥*Departamento de Biologia Funcional-Instituto Universitario de Oncologia del Principado de Asturias, Oviedo, Spain, and* ⊥*Instituto de Biologia Molecular de Barcelona, CSIC, Parc Cientific de Barcelona, Barcelona, Spain*

*Received August 30, 2010; Revised Manuscript Received October 27, 2010*

ABSTRACT: The antitumor antibiotics mithramycin A and chromomycin $A_3$ bind reversibly to the minor groove of G/C-rich regions in DNA in the presence of dications such as $Mg^{2+}$, and their antiproliferative activity has been associated with their ability to block the binding of certain transcription factors to gene promoters. Despite their biological activity, their use as anticancer agents is limited by severe side effects. Therefore, in our pursuit of new structurally related molecules showing both lower toxicity and higher biological activity, we have examined the binding to DNA of six analogues that we have obtained by combinatorial biosynthetic procedures in the producing organisms. All these molecules bear a variety of changes in the side chain attached to C-3 of the chromophore. The spectroscopic characterization of their binding to DNA followed by the evaluation of binding parameters and associated thermodynamics revealed differences in their binding affinity. DNA binding was entropically driven, dominated by the hydrophobic transfer of every compound from solution into the minor groove of DNA. Among the analogues, mithramycin SDK and chromomycin SDK possessed the higher DNA binding affinities.

Mithramycin A (MTA), also known as plicamycin, and chromomycin $A_3$ (CRO) are aureolic acid-type polyketide antibiotics produced by *Streptomyces argillaceus* (ATCC 12596) and *Streptomyces griseus* subsp. *griseus* (ATCC 31053), respectively (*1*). They contain the same tricyclic core moiety but differ in the nature of their oligosaccharide chains (Figure 1). These structural dissimilarities impart subtle differences in their binding to DNA (*2*) that might be at the origin of their different biological activity profiles (*1*, *3*). MTA has been used in the treatment of Paget's disease and advanced testicular carcinoma (*4*), while CRO has been used in Japan against advanced stomach cancers (*5*); however, they exhibited severe toxic side effects that have limited their clinical use. Recently, the use of these molecules as therapeutic agents is re-emerging in both cancer- and non-cancer-related diseases (*6*−*9*). Given the toxicity of MTA and CRO, the availability of analogues showing both lower toxicity and higher biological activity opens new possibilities for therapeutic applications.

The activity of the aureolic acid group of compounds has been associated with their ability to bind to G/C-rich DNA regions via the minor groove (*10*−*14*). Divalent cations such as $Mg^{2+}$ are essential requirements for the association with DNA at and above physiological pH (*15*−*17*). Because of their binding to DNA, these compounds can inhibit transcription both in vivo and in vitro (*18*−*21*). The sequence-selective binding of MTA and CRO to DNA is basically attained through direct hydrogen bonding between the 8-*O*-hydroxyl group in the antibiotic molecules and the 2-amino group of the guanine at GpC or GpG steps, while their respective trisaccharide moieties are essential for optimal binding (*2*, *14*, *22*). The thermodynamic analysis of the binding of MTA and CRO to DNA has shown that this is entropically driven (*16*, *23*), dominated by the hydrophobic transfer of the $Mg^{2+}$-coordinated compound dimers from solution to the DNA binding site (*23*). Moreover, hydrogen bonding plays a part in the binding of the oligosaccharide chains along the minor groove (*2*, *13*, *22*, *24*).

The genetic organization of the MTA and CRO biosynthesis gene clusters has been studied in detail by gene sequencing, insertional inactivation, and gene expression (*1*, *11*, *25*−*29*). Furthermore, most of the biosynthetic intermediates in these pathways have been isolated and characterized, and some of them have shown enhanced antitumor activity (*11*, *19*, *20*, *25*, *29*).

Here, we have examined whether six analogues of MTA or CRO (Figure 1), which we obtained by combinatorial biosynthetic procedures in the producing organisms, may bind to DNA with different affinities. These biosynthetically produced antibiotics exhibit an array of structural changes in the highly functionalized pentyl side chain attached at the 3-position in MTA and CRO (Figure 1). Changes in the alkyl C-3 side chain of MTA or CRO have been characterized less than their common chromophore and the different oligosaccharide chains. The experimental determination of the apparent binding constant of a drug for its target molecule is of considerable importance, and it represents a basic experimental parameter in the prediction

†This work was supported by grants from the Spanish Ministry of Science and Innovation (BFU2010-15518 and BFU2007-60998) and the FEDER program of the European Community (to J.P.) and from "Red Temática de Investigación Cooperativa de Centros de Cáncer" (Ministry of Health, Spain; ISCIII-RETIC RD06/0020/0026) (to J.A.S.).

*To whom correspondence should be addressed: Instituto de Biologia Molecular de Barcelona, CSIC, Parc Científic de Barcelona, Baldiri Reixac, 10, E-08028 barcelona, Spain. Phone: +34 93 4034959. Fax: +34 93 4034979. E-mail: jpmbmc@ibmb.csic.es.


Published on Web 11/10/2010

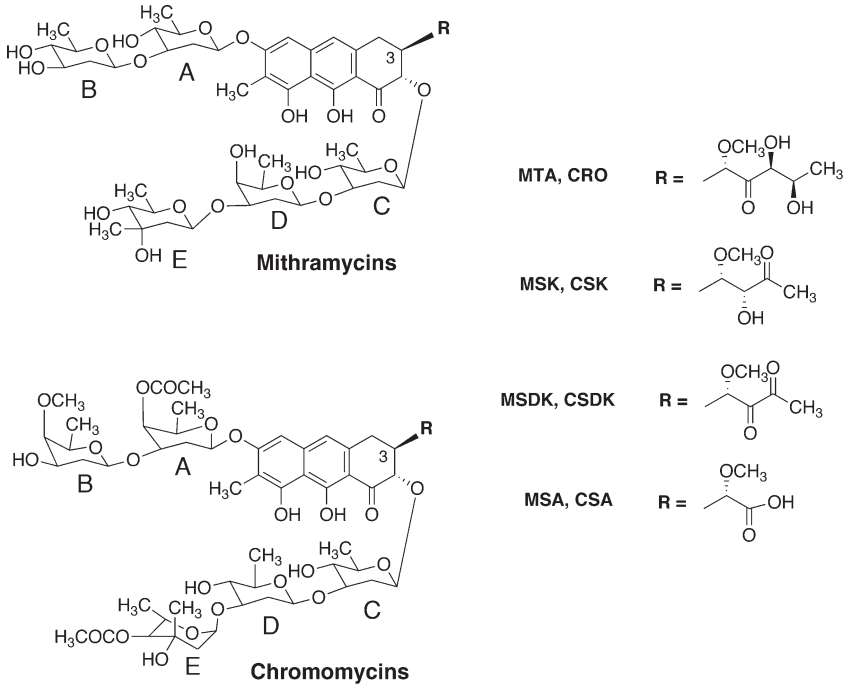


FIGURE 1: Chemical formulas of mithramycins and chromomycins. Mithramycin A (MTA), mithramycin SK (MSK), mithramycin SDK (MSDK), mithramycin SA (MSA), chromomycin $A_3$ (CRO), chromomycin SK (CSK), chromomycin SDK (CSDK), and chromomycin SA (CSA).

of drug efficiency and drug interactions (*30*). We have observed that mithramycin and chromomycin analogues exhibit differences in the magnitude of their binding to DNA that might depend on the exact composition of their respective side chains attached at C-3 as well as of the different oligosaccharide chains that differentiate mithramycins from chromomycins (Figure 1). For all the compounds, the binding to DNA was entropically driven, dominated by the hydrophobic transfer of every compound from solution into the duplex binding site, while hydrogen bonding and other noncovalent contacts of the peculiar polyketide chains may also participate in the sequence-selective binding of the analogues.

## MATERIALS AND METHODS

*Mithramycins and Chromomycins*. Mithramycin A (MTA), mithramycin SK (MSK), mithramycin SDK (MSDK), mithramycin SA (MSA), chromomycin $A_3$ (CRO), chromomycin SK (CSK), chromomycin SDK (CSDK), and chromomycin SA (CSA) (Figure 1) were isolated and purified from the producing organisms as described previously (*11*, *25*), and their purity (≥95%) was checked by high-performance liquid chromatography (HPLC). Stock solutions (500 $\mu$M) of the different compounds were prepared in 80 mM NaCl and 20 mM Hepes (pH 7.0) (designed HES buffer), kept at −20 °C, and diluted to the desired concentration before the experiments. The concentrations of the different compounds were determined by using the molar extinction coefficients described elsewhere (*11*, *16*, *17*, *25*). When required for the different experiments (see Results), $MgCl_2$ was added to HES buffer to a final concentration of 200 $\mu$M, 1.5 mM, or 11 mM.

DNA from salmon testes (Sigma), with G+C content of ~42%, was dissolved in HES buffer, sonicated, extracted with phenol, and dialyzed twice against the same buffer. The DNA concentration (in base pairs) was determined spectrophotometrically by using a molar extinction coefficient of 12820 $M^{-1}$ $cm^{-1}$ at 260 nm.

Table 1: Spectroscopic Characteristics of DNA−Antibiotic Complexes[a]

| | | fluorescence | | absorption | |
|---|---|---|---|---|---|
| | [$MgCl_2$] ($\mu$M) | $\lambda_{ex}$ (nm) | $\lambda_{em}$ (nm) | $\lambda_{max}$ (nm) | isosbestic point (nm) |
| MTA | 200 | 470 | 554 | 402 | 413 |
| | 1500 | 470 | 557 | 410 | 417 |
| MSK | 200 | 440 | 543 | 401 | 417 |
| | 1500 | 440 | 546 | 401 | 417 |
| MSDK | 200 | 420 | 548 | 407 | 415 |
| | 1500 | 420 | 564 | 416 | 432 |
| MSA | 200 | 410 | 566 | 417 | 447 |
| | 1500 | 410 | 570 | 420 | 445 |
| CRO | 200 | 460 | 555 | 405 | 414 |
| | 1500 | 460 | 555 | 407 | 414 |
| CSK | 200 | 440 | 555 | 406 | 414 |
| | 1500 | 440 | 555 | 411 | 414 |
| CSDK | 200 | 420 | 560 | 405 | 413 |
| | 1500 | 420 | 560 | 410 | 413 |
| CSA | 200 | 410 | 560 | 412 | 444 |
| | 1500 | 410 | 562 | 419 | 446 |

[a]Experiments were undertaken in HES buffer [80 mM NaCl and 20 mM Hepes (pH 7.0)] at 25 °C in the presence of the listed $MgCl_2$ concentrations.

*Spectroscopic Analyses*. Absorption and fluorescence spectroscopy experiments were conducted at 25 °C in a Cary300 Bio UV−visible spectrophotometer (Varian Inc.) or a Jasco VP-650 spectrophotometer, and in a Cary Eclipse fluorescence spectrophotometer (Varian Inc.), using 1 cm path length cuvettes. For fluorescence measurements, excitation wavelengths were selected within the 410−470 nm range, depending of the antibiotic studied, to avoid photodegradation that may occur at the absorption maxima, while emission wavelengths were in the 550−570 nm range (Table 1); 4 nm slit widths were used.

Circular dichroism (CD) measurements were taken in a Jasco J-810 spectropolarimeter in 1 cm path length cuvettes. The wavelengths studied ranged from 240 to 320 nm. Scans were recorded

at 1 nm intervals. A scan of buffer alone was recorded to provide a baseline. A solution containing 20 $\mu$M DNA (bp) was titrated by addition of aliquots of 4 M $MgCl_2$, and following a 2 h incubation, the CD spectra were recorded at 25 °C. Molar ellipticities were calculated in terms of the DNA concentration (base pairs) corrected by dilution.

*DNA Binding Assays*. Binding constants were determined by fluorescence titration. Solutions (20 $\mu$M) of the different mithramycins and chromomycins dissolved in HES buffer containing either 200 $\mu$M or 1.5 mM $MgCl_2$ were incubated for 1 h at room temperature to ensure the $Mg^{2+}$-mediated dimerization of the compounds. Small aliquots of DNA in the same buffer were added to compound solutions, and the fluorescence was measured after a 3 min equilibrium. The background fluorescence emission was $< 3\%$ of the maximum. No correction was undertaken for optical filtering effects because the absorbance of the samples at $\lambda_{max}^{vis}$ did not exceed 0.03. Experimental points for binding isotherms were fitted by nonlinear curve fitting. The apparent (observed) binding constant ($K_{obs}$) was calculated by using the following equation (*31*):

$$1/\Delta F = 1/\Delta F_{max} + 1/[K_{obs}\Delta F_{max}(Cd - Co)] \quad (1)$$

where Cd is the concentration of DNA (base pairs) and Co is the initial concentration of the ligand. $\Delta F$ is the change in fluorescence emission intensity at the emission wavelength upon addition of each aliquot of DNA, and $\Delta F_{max}$ is the same parameter when the compound is totally bound to DNA.

A linear plot of $1/\Delta F$ versus $1/(Cd - Co)$ was used to obtain $\Delta F_{max}$ and $K_{obs}$ (*32*). The approach is based on the assumption that the emission intensity is linearly proportional to the concentration of the ligand, and under the experimental condition $Cd \gg Co$. Both conditions were fulfilled in our experiments by working with 20 $\mu$M compound and an at least 4-fold excess of DNA.

The binding stoichiometry of the DNA−-compound complexes ($n$), in terms of number of DNA base pairs covered per $Mg^{2+}$-coordinated antibiotic dimer, was estimated from the intersection of two straight lines of the normalized increase in fluorescence versus the ratio of the input concentrations of DNA (base pairs) and antibiotic.

*Estimation of Thermodynamic Parameters*. Free energies were calculated from the experimental binding constants ($K_{obs}$) calculated at 25 °C by the standard relation:

$$\Delta G = -RT \ln K_{obs} \quad (2)$$

Linear least-squares fits of ln $K_{obs}$ versus $1/T$ were used to estimate the enthalpy change ($\Delta H$) from the slope according to the van't Hoff relationship:

$$[\partial(\ln K)/\partial(1/T)] = -\Delta H/RT \quad (3)$$

The binding entropy ($\Delta S$) was evaluated using the standard thermodynamic relationship

$$\Delta S = (\Delta H - \Delta G)/T \quad (4)$$

*Molecular Modeling of DNA−Compound Complexes*. Models of MSK, MSDK, and MSA molecules were built on MTA−DNA coordinates taken from published NMR studies (Protein Data Bank entry 146D) (*14*), whereas those of CSK, CSDK, and CSA were based upon a CRO−oligonucleotide X-ray structure (Protein Data Bank entry 1VAQ) (*22*). Initial models were manually built using CHIMERA (*33*) and PYMOL (http://www.pymol.org). The geometry of these models was optimized using the general amber force field (GAFF) for organic molecules (*34*) in the antechamber module of AMBER version 9 (*35*).

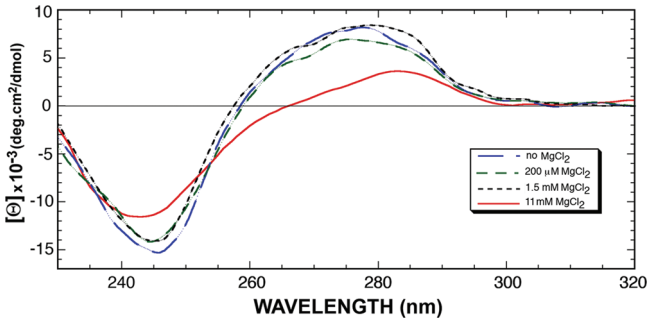


FIGURE 2: Circular dichroism spectra of salmon testes DNA in HES buffer and in the presence of 200 $\mu$M, 1.5 mM, and 11 mM $MgCl_2$ in the same buffer.

## RESULTS

*Interaction of Aureolic Acid Antibiotics and Salmon Testes DNA with $Mg^{2+}$*. Because the interaction of MTA and CRO with DNA requires the presence of divalent ions, such as $Mg^{2+}$, we first examined whether the concentration of magnesium used [or the molar ratio of $Mg^{2+}$ to DNA (base pairs)] has an effect on DNA conformation, the $Mg^{2+}$-coordinated antibiotic dimers, or DNA−ligand interactions. Figure 2 shows that 200 $\mu$M or 1.5 mM $MgCl_2$ had no effect on the conformation of salmon testes DNA. Nevertheless, higher $MgCl_2$ concentrations, up to 11 mM, resulted in changes in the CD spectra: the magnitude of the long-wavelength positive CD band decreased with a shift in the 258 nm crossover to longer wavelengths. Both the increase in ionic strength (produced by $MgCl_2$, because the $Na^+$ concentration was kept constant) and a dehydration produced by a large excess of magnesium ions (11 mM $MgCl_2$) with respect to the DNA concentration [20 $\mu$M (base pairs)] could induce the changes observed. The types of CD changes shown in Figure 2, including those found around the 245 nm region, were consistent with the fact that some regions of DNA were undergoing a B- to A-DNA conformational transition (*36*).

The effects of the $Mg^{2+}$ concentration on the dication-mediated dimerization of the antibiotics were explored in HES buffer containing a variety of $MgCl_2$ concentrations up to 11 mM. UV−visible spectroscopy was used to determine the influence of magnesium upon the dimerization of the different aureolic acid antibiotics in HES buffer (i.e., in the presence of 100 nM $Na^+$). Figure S1 (Supporting Information) displays the effect of increasing $MgCl_2$ concentrations on the compound spectra. For all the analogues, their spectra changed depending on the $MgCl_2$ concentration. This experimental observation was consistent with the fact that dications can bind to aureolic acid antibiotics in the absence of DNA (*16*, *17*, *37*); thus, $Mg^{2+}$-mediated dimerization of the different compounds took place. In the presence of 200 $\mu$M or 1.5 mM $MgCl_2$, corresponding to a $Mg^{2+}$:antibiotic molar ratio of 10 or 75, respectively, there was a broadening and slight red shift in the absorbance maxima (Figure S1 of the Supporting Information and Table 1). This red shift became even more evident when higher (11 mM $MgCl_2$) concentrations were used, which corresponded to a $Mg^{2+}$:antibiotic molar ratio of 550.

*Binding Affinity and Stoichiometry of DNA−Antibiotic Interactions*. Changes in the visible absorption spectra of the

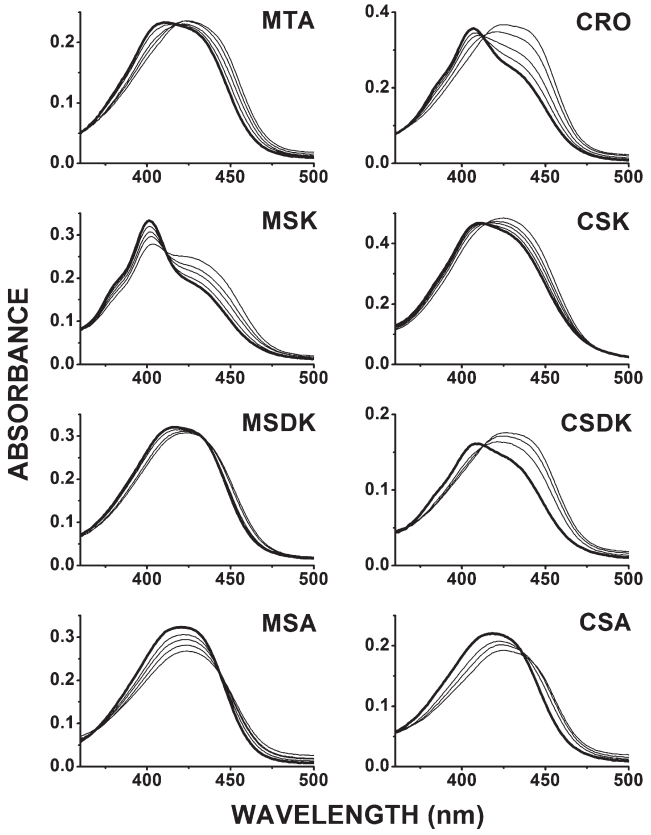


FIGURE 3: Optical absorbance spectra of the complexes formed between the $Mg^{2+}$-coordinated antibiotic dimers and DNA in HES buffer containing 1.5 mM $MgCl_2$ at 25 °C. The different complexes correspond to the titration of 20 $\mu$M antibiotic (thick line) with 25, 75, 150, and 250 $\mu$M salmon testes DNA (thin lines).

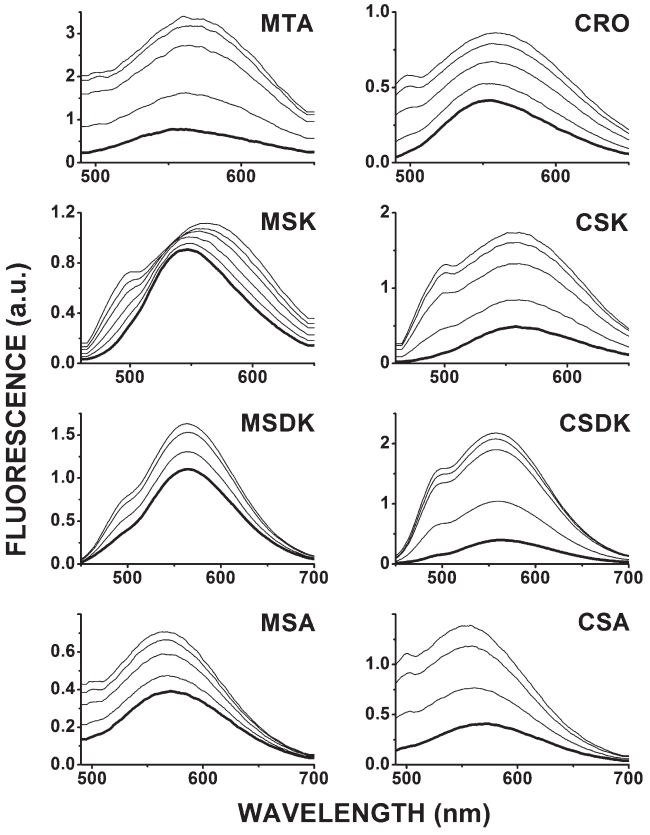


FIGURE 4: Fluorescence spectra of the complexes formed between the $Mg^{2+}$-coordinated antibiotic dimers and DNA in HES buffer containing 1.5 mM $MgCl_2$ at 25 °C. The different complexes correspond to the titration of 20 $\mu$M compound (thick line) with 25, 75, 150, and 250 $\mu$M salmon testes DNA (thin lines).

different mithramycins and chromomycins upon addition of DNA demonstrated the association of the $Mg^{2+}$-coordinated antibiotic dimers with DNA (Table 1 and Figure 3). In general, single isosbestic points were observed in the presence of 200 $\mu$M $MgCl_2$ (Figure S2 of the Supporting Information) and more unambiguously in 1.5 mM $MgCl_2$ (Figure 3), which supported the analysis of binding in terms of the free and single type of bound ligand. However, among the analogues, MSA and CSA did not generate unique isosbestic points at any $MgCl_2$ concentration.

The fluorescence properties of the $Mg^{2+}$-coordinated dimers of the different analogues were used to quantify their binding to DNA. Figure 4 shows representative examples of the dequenching of the fluorescence of the compounds that occurred upon their interaction with DNA in the presence of 1.5 mM $MgCl_2$. The experiments conducted in 200 $\mu$M $MgCl_2$ are shown in Figure S3 (Supporting Information). These changes in fluorescence were used to evaluate binding constants (Figure 5) and the binding stoichiometry (Figure 6), as described in Materials and Methods. Fluorescence titrations were performed using fixed concentrations of the compounds (20 $\mu$M), such that $1/K_b$ values were on the same order of magnitude as the ligand concentration to obtain well-defined binding isotherms. Table 2 summarizes the binding parameters obtained for all the compounds in HES buffer containing either 200 $\mu$M or 1.5 mM $MgCl_2$.

Binding stoichiometries ($n$) determined for all the antibiotics were in the range of 4−6 (Table 2), consistent with the size of the binding sites inferred from NMR and crystallographic studies (*14*, *22*). The variability we observed in the stoichiometry values could reflect small differences in the disposition of the different

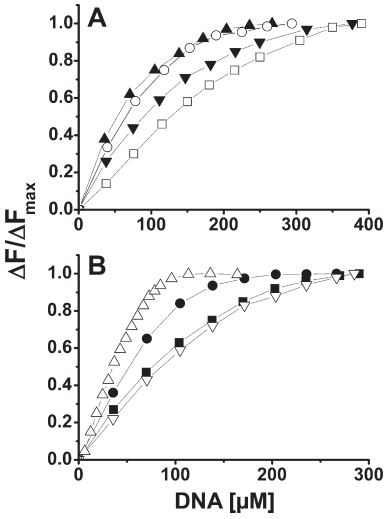


FIGURE 5: DNA binding analyses. (A) Comparative fluorescence titration curves for the binding of MTA (○), MSK (▼), MSDK (▲), and MSA (□) to salmon testes DNA in HES buffer containing 1.5 mM $MgCl_2$ at 25 °C. (B) Comparative fluorescence titration curves for CRO (△), CSK (■), CSDK (●), and CSA (▽). Other details as in panel A. $\Delta F/\Delta F_{max}$ represents the normalized increase in fluorescence, where $\Delta F$ corresponds to the change in fluorescence emission intensity after each addition of DNA with respect to the free ligand and $\Delta F_{max}$ the maximum value. Connecting curves were obtained by nonlinear fitting of the experimental data.

analogues in the minor groove. Changes in the C-3 chain among the different analogues resulted in quantitative differences in their

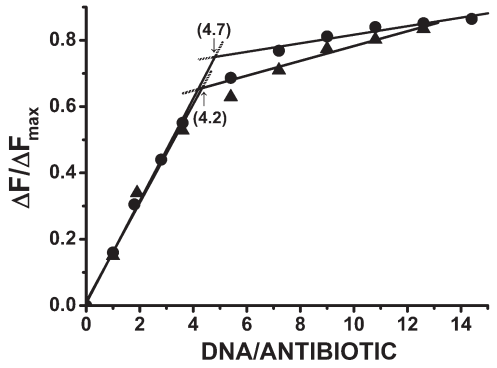


FIGURE 6: Binding stoichiometries ($n$) in terms of the number of DNA base pairs covered per $Mg^{2+}$-coordinated antibiotic dimer, calculated at the intersection of the two straight lines in the plot of normalized fluorescence ($\Delta F/\Delta F_{max}$) vs the molar ratio of DNA (base pairs) vs antibiotic. This figure presents results of the experiments performed with MSDK (▲) and CSDK (●). The $n$ values for all the analogues are listed in Table 2.

Table 2: Summary of the Binding Parameters for the Interaction of $Mg^{2+}$-Coordinated Antibiotic Dimers with Salmon Testes DNA[a]

| | 200 $\mu$M $MgCl_2$ | | 1.5 mM $MgCl_2$ | |
|---|---|---|---|---|
| | $K_{obs}$ ($\times 10^4$ $M^{-1}$) | $n^b$ | $K_{obs}$ ($\times 10^4$ $M^{-1}$) | $n^b$ |
| MTA | $1.5 \pm 0.1$ | 4.9 | $1.7 \pm 0.1$ | 4.7 |
| MSDK | $2.1 \pm 0.2$ | 4.7 | $2.2 \pm 0.1$ | 4.2 |
| MSK | $0.95 \pm 0.15$ | 4.7 | $1.2 \pm 0.1$ | 4.2 |
| MSA | $0.50 \pm 0.10^c$ | 4.5 | $0.64 \pm 0.03^c$ | 5.7 |
| CRO | $4.5 \pm 0.4$ | 4.0 | $4.7 \pm 0.4$ | 4.6 |
| CSDK | $2.1 \pm 0.2$ | 4.8 | $3.0 \pm 0.3$ | 4.7 |
| CSK | $1.5 \pm 0.1$ | 5.3 | $1.6 \pm 0.1$ | 5.2 |
| CSA | $0.5 \pm 0.2^c$ | 5.7 | $1.2 \pm 0.2^c$ | 5.3 |

[a]Values were determined from spectrofluorometric titrations in HES buffer at 25 °C (see Figure 4). Data are means ± the standard deviation for four independent experiments. [b]Stoichiometry of binding in terms of the number of DNA base pairs covered per $Mg^{2+}$-coordinated antitumor dimer. [c]For these analogues, the presence of unique isosbestic points cannot be unambiguously established.

binding to DNA. Although MSA and CSA bind to DNA regardless of the acidic characteristics of the alkyl chain linked to C-3 (Figure 1), the quantitative values listed in Table 2 should be taken with skepticism because the binding of these two molecules did not seem to meet the two-state reaction required for our quantitative approach, for which the appearance of a clear (unique) isosbestic point is mandatory for the determination of a meaningful binding curve. In summary, the strength of binding to DNA of mithramycins was in the following order: MSDK > MTA > MSK > MSA. For chromomycins the order was as follows: CRO > CSDK > CSK > CSA. The ranking of the reliable $K_b$ for all the compounds was as follows: CRO > CSDK > MSDK > MTA = CSK > MSK. MSA and CSA were not considered for the reasons stated above.

*Effects of $Mg^{2+}$ on the Binding of Mithramycin and Chromomycin to DNA*. The apparent binding constants, documented in Table 2, depended on the final concentration of $MgCl_2$. The differences reflected the effect of the ionic strength on DNA binding plus a more located effect of $Mg^{2+}$ on DNA and/or on the different analogues. The $Mg^{2+}$-coordinated dimers of the different aureolic acid antibiotics are uncharged species at neutral pH (except MSA and CSA that bear a terminal acidic group in the C-3 chain). We have previously shown that changes in NaCl concentration have an only small effect on the binding of MTA or MSK to DNA (*23*).

The presence of $Mg^{2+}$ in the binding buffer merits further consideration not only because of the effects on the ionic strength but also because of the direct binding (condensation) of the dication to the DNAs (*38*). The effect of multivalent cations on the DNA−ligand interactions is greater than expected on the basis of their contribution to the ionic strength (*38*, *39*). All the assays were performed in the presence of 100 mM $Na^+$ to minimize the difficulties that the presence of the dication can produce in the interpretation of our binding data. The presence of $Na^+$ would facilitate the solubility of the compound and reduced its level of self-association, while the concentrations of $MgCl_2$ were kept relatively lower; thereby, the contribution of $Mg^{2+}$ to the ionic strength was minimized as much as possible. In all cases, the final concentration of $Mg^{2+}$ was never higher than 1.5 mM in the presence of DNA. Hence, any effects of the dications because of their direct binding to DNA were reduced, including the dehydration of the double helix produced by bound dications (*39*).

To gain further insights into the differences in the binding of the aureolic acid antibiotics to DNA, we undertook a molecular modeling approach to explore the fitting of the different aureolic acid molecules into the minor groove of DNA, and whether differences in potential hydrogen bonding and other noncovalent interaction contacts can occur between the alkyl chains at C-3 of the tricyclic core moiety and the DNA minor groove. The molecular modeling illustrations shown in Figure 7 indicate that the different C-3 side chains can be accommodated without a large disruption of the interaction of the rest of the molecule with DNA. Therefore, differences in the binding between chromomycins and mithramycins provided by other structural components of the compound would remain almost unaltered. Besides, Figure 7 illustrates that every analogue can present a varied pattern of interactions between the C-3 groups and the DNA backbone, which might play a part in the differences in the strength of binding to DNA that we observed experimentally (Table 2). Among the analogues, the alkyl chains linked to the C-3 position differ from that common to MTA and CRO in both their length (all the variants being shorter than the original chains) and the distribution of polar atoms that can act as potential donors or acceptors in hydrogen bonding (cf. Figures 1 and 7). All the analogues lack the 4′-hydroxyl found in MTA and CRO, whereas carbonyl groups in the SK and SDK analogues replace the 3′-hydroxyl. MSK and CSK bear a hydroxyl group instead of the 2′-carbonyl. In MSDK and CSDK, which do not bear hydroxyl groups, the C-3 chain provided hydrogen bond acceptor groups but not hydrogen bond donors. The alkyl 3-side chain of MSK and CSK contained both hydrogen bond donor and acceptor functions, yet the potential donor group was located where MTA, or CRO, and MSDK, or CSDK, bear a carbonyl as a potential hydrogen bond acceptor. Figure 7 illustrates that the repositioning of the various functional groups in the side chains of the SDK and SK analogues, compared to MTA or CRO, allowed differences in the DNA binding characteristics of these molecules. Moreover, the shortest derivatives MSA and CSA end in carboxylic groups that could not be accommodated next to the DNA polyphosphate chains because they were negatively charged at neutral pH. Notwithstanding the differences in the involvement of the C-3 side chains in binding to DNA, the stronger binding of the chromomycins compared to that of their counterpart mithramycins (Table 2) might be

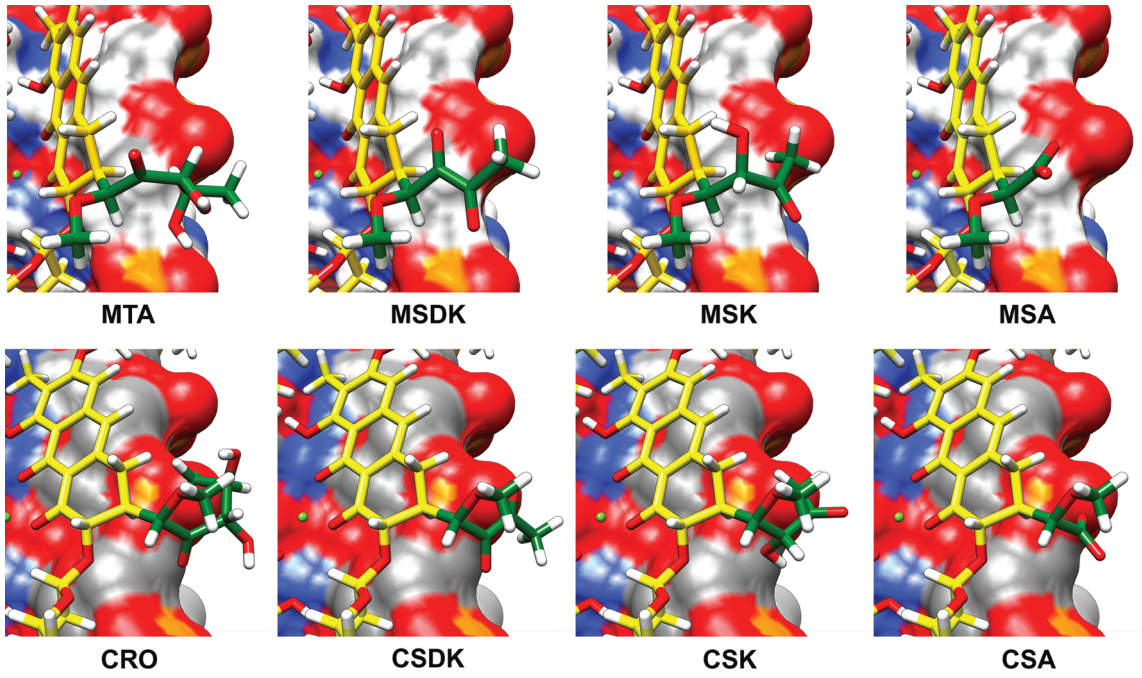


FIGURE 7: Differences in the binding to DNA of the alkyl chains linked to C-3 in the different mithramycin and chromomycin analogues. Part of the DNA minor groove is exposed to the viewer, with the sugar−phosphate backbone of one of the DNA chains at the right. The figure shows close-ups of the tricyclic chromophores and of the respective C-3 groups of MTA, MSDK, MSK, and MSA (top panel) and CRO, CSDK, CSK, and CSA (bottom panel). The DNA molecular surface is colored by element (gray for carbon, red for oxygen, and blue for nitrogen). In each case, the chromophore and C-3 chains of one of the monomers are represented, with the beginning of the oligosaccharide chains pointing up- and downward. The different compounds are also colored by element, but in this case with carbons colored yellow, except for the C-3 alkyl chain, where they are colored green, with the hydrogens colored white. The $Mg^{2+}$ ions that participate in the dimerization of the different compounds are displayed as a green sphere.

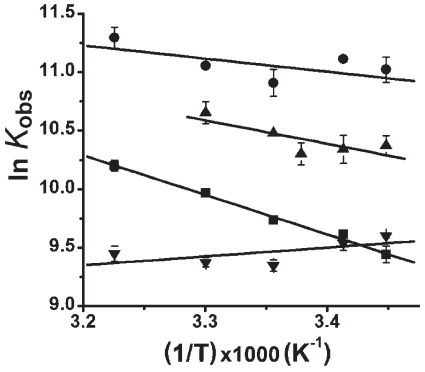


FIGURE 8: Sample van't Hoff plots for the interaction of $Mg^{2+}$-coordinated antibiotic dimers with salmon testes DNA in HES buffer containing 1.5 mM $MgCl_2$: MSDK (▲), CSDK (●), MSK (▼), and CSK (■). Values are means ± the standard deviation of three independent experiments. Solid lines correspond to the linear least-squares fits of the experimental data (see also Table 3).

achieved through the binding of the rest of the molecule within the minor groove, which is in part lined by the presence of two acetoxy groups in the A and E sugars of the chromomycins (Figure 1). In this regard, a comparison of the top and bottom panels in Figure 7 reveals some differences in the orientation of the chromophores between mithramycins and chromomycins.

*Evaluation of Thermodynamic Parameters*. van't Hoff plots derived from the binding constants determined at different temperatures for several mithramycin and chromomycin analogues are shown in Figure 8, and the values of the thermodynamic parameters for MSK, MSDK, CSK, and CSDK are summarized in Table 3. For all these molecules, the enthalpies were small and positive, except for MSK that exhibited a low negative value.

Table 3: Thermodynamic Parameters for the Binding of $Mg^{2+}$-Coordinated Antibiotic Dimers to Salmon Testes DNA[a]

| | $\Delta G$ (25 °C) (kcal/mol) | $\Delta H$ (25 °C) (kcal/mol) | $T\Delta S$ (25 °C) (kcal/mol) |
|---|---|---|---|
| MSDK | −6.1 | 0.31 | 6.4 |
| MSK | −5.5 | −0.14 | 5.4 |
| CSDK | −6.5 | 0.20 | 6.7 |
| CSK | −5.6 | 0.57 | 6.2 |

[a]Values were determined from van't Hoff plots of the variation in binding constant calculated from spectrofluorimetric titration data as a function of temperature (Figure 8).

Binding to DNA was entropically driven for all these molecules (Table 3). The moderately negative enthalpy calculated for the MSK interaction was at variance with our previous calorimetric determinations of a small positive value (*23*). This probably indicates that, within the experimental error inherent to a van't Hoff analysis of the data (*40*), we were dealing with molecules for which the net enthalpic term of binding to DNA was close to zero. These observations can be considered a sign that some hydrogen bonds gained upon ligand binding to C/G-rich DNA regions were somewhat compensated by the loss of hydrogen bonds from displaced water. Furthermore, our results highlight the bias in the van't Hoff enthalpy estimates in DNA−drug interactions resulting from heat capacity ($\Delta C_p$) effects that can be precisely detected by isothermal calorimetry (*40*, *41*). So far, our more reliable estimates of $\Delta H$ and $\Delta S$ obtained to date for aureolic acid antibiotics [for MTA by ITC (*23*)] would agree with the fact that a rather small positive enthalpy and an overwhelming entropy term (Table 3) produced the free energy of binding for most, if not all, of the mithramycin and chromomycin analogues.

## DISCUSSION

The great improvement in our understanding of the synthetic pathways by which some microorganisms produce antibiotics, including those with cytotoxic or cytostatic profiles, has encouraged the manipulation of the antibiotic gene clusters to obtain new molecules. This approach, named combinatorial biosynthesis, has been used to alter genes in the biosynthesis pathways of the aureolic acid antibiotics to produce a variety of analogues with potentially improved activity (*1*, *29*). The therapeutic use of two of these molecules (MTA and CRO) is limited by their induction of severe side effects (*4*); thereby, the availability of new analogues can provide us with molecules having improved pharmacological profiles. In this paper, we have quantified the binding to DNA of six of these analogues (MSK, MSDK, MSA, CSK, CSDK. and CSA) that we have obtained by combinatorial biosynthesis in the producing organisms, together with the parental MTA and CRO molecules (Figure 1).

DNA binding studies have endowed us with fundamental information for the understanding of subtle differences in the binding of different mithramycin and chromomycin analogues, which provide basic experimental parameters for the prediction of drug interactions. The molecules examined here differ in the side chains attached at the C-3 position of their common tricyclic chromophore, which offers the opportunity to investigate the relevance that changes in this chain may have in DNA binding. Several molecular interactions between hydroxyl and carbonyl groups in this chain have been shown to participate in the binding of MTA and CRO to DNA (*2*, *14*, *22*). Moreover, some of the changes in the chain attached to C-3 have been correlated with improved biological profiles (*3*, *11*, *19*, *25*, *42*, *43*).

The experiments described here have been undertaken in HES buffer, which contains 100 mM $Na^+$, and to which $MgCl_2$ was added to a final concentration of 200 $\mu$M or 1.5 mM. Previous spectroscopic data on MTA and CRO were obtained in the absence of NaCl and over 10 mM $MgCl_2$ (*16*, *17*). The rather high concentrations of magnesium used in those studies make difficult the comparison with the $K_b$ values reported here (Table 2). The $K_b$ values reported by Aich and co-workers for the binding of MTA and CRO to heterogeneous DNA are higher than those we present here (*16*, *17*), while the stoichiometries are very similar within experimental error. It is worth noting that the presence of both $Na^+$ and $Mg^{2+}$ imparted unusual characteristics to the binding of the drug to DNA, which differed from those that are determined by the ionic strength effect, because of the complex effects of counterions of different valence that include differences in the binding of either $Na^+$ or $Mg^{2+}$ to DNA (*38*, *44*). For example, the binding of $Mg^{2+}$, which causes more efficient charge neutralization, is enthalpically more favorable than that of $Na^+$ (*39*).

We have observed quite similar $K_b$ values for the different compounds regardless of the presence of 200 $\mu$M or 1.5 mM $MgCl_2$ (Table 2), indicating that equivalent complexes were formed at either $MgCl_2$ concentration. This was in contrast with the two types of complexes previously reported to be involved in the binding of MTA or CRO to DNA in the absence of $Na^+$, which seemed to depend on the $MgCl_2$ concentration (*16*, *17*, *45*). Under the experimental conditions reported here, the unique species binding to DNA at relatively low $MgCl_2$ concentrations, in the presence of 100 mM $Na^+$, are $Mg^{2+}$-coordinated antibiotic dimers. This observation is in keeping with the unique mode of binding of MTA to DNA determined by isothermal titration calorimetry (ITC) (*23*).

The differences in DNA binding affinity among the analogues reflect the changes in the alkyl chain at C-3 of the chromophore (Figure 7). Additionally, the peculiar oligosaccharides that distinguish the mithramycin and chromomycin families might determine the size of the binding site (*32*) and the flexibility of the molecules (*2*, *32*). The main difference is the presence of acetoxy groups in the A and E sugars of CRO, and its analogues, which participate in additional hydrogen bonding (*2*). This would explain why, in general, chromomycins bind to DNA more strongly than their mithramycin analogues (Table 2).

All the aureolic acid antibiotics examined here should target similar G/C-rich regions in the DNA minor groove, mainly because they bear the same tricyclic chromophore, which is known to play a key role in sequence-specific recognition (*2*, *14*, *22*, *46*). The small binding enthalpies (Table 3) would suggest that hydrogen bonding and van der Waals contacts play only a small role in stabilizing the drug−DNA complexes. Nevertheless, the formation of specific hydrogen bonds between the 8-*O*-hydroxyl groups, conserved among the analogues, and the 2-amino group of the guanine at GpC or GpG steps has a central role in sequence-selective binding to DNA (*13*, *22*, *24*). By exploring the restriction enzyme cleavage of the different DNA−compound complexes, we reported beforehand that subtle differences exist in the sequence of the C/G-rich tracts specifically recognized by the different analogues (*3*), which could not be easily detected by footprinting (*42*).

As mentioned above, differences in binding affinity among the analogues might arise from some binding particularities provided by the different side chains linked to C-3. Given the repositioning of the analogues in the C-3 side chains of the SDK, SK, and SA derivatives compared to the parental MTA and CRO, one can envisage differences in the DNA binding mode of the analogues (Figure 7) consistent with the diversity of binding constants listed in Table 2. In MSK and CSK, the C-3 chain bears both hydrogen bond donor and acceptor functions, but the potential donor group is in a position where both MTA or CRO and MSDK or CSDK have a carbonyl, a potential hydrogen bond acceptor. MSA and CSA contain carboxyl groups at the end of the C-3 side chain, which are negatively charged at neutral pH and, therefore, can impede their location near the polyphosphate chains. This feature could account for the absence of clear (unique) isosbestic points (Figure 3 and Figure S2 of the Supporting Information) because of the absence of a lone orientation of the MTA or CSA molecules bound to DNA.

Although only a deeper analysis of the dynamics of the interactions between every analogue and DNA has the potential to unveil the molecular details that may cause such differences, it is tempting to conclude that two kinds of phenomena may be involved in the differences in the strength of DNA binding among the analogues. On one hand, the diverse distribution of hydrogen donors and acceptors could produce different patterns of hydrogen bonding, as well as of other nonbonded contacts, with varying lifetimes. Nevertheless, those molecular interactions appeared to contribute little to the free energy of binding (Table 3 and ref *23*), which would indicate that hydrogen bonds participate in a nearly isoenergetic process in which water, or ions, bound to DNA are replaced by hydrogen bonding with the C-3 alkyl chains, in keeping with similar observations for other minor groove binders (*41*). On the other hand, the less bulky nature of the alkyl C-3 chains in the analogues may also subtly affect the position of the tricyclic chromophore in the minor groove of DNA (Figure 7), a disposition in which differences in the sugar moieties between chromomycins

and mithramycins would make the latter more flexible and less sensitive to the dimensions of the minor groove (*2*).

For the $Mg^{2+}$-coordinated dimers of the different compounds, the free energy of binding ($\Delta G$) was negative (favorable), as a consequence of various positive entropic contributions to binding in the minor groove, which include ions and water release (*23*, *41*, *47*), as well as "hydrophobic" interactions. In any case, the positive entropic term was enough to counterbalance the unfavorable entropic cost of forming DNA−compound complexes. The large entropic term and the positive (small) enthalpies of binding (Table 3 and refs *16*, *17*, and *23*) imply an entropically driven binding process, which has been considered a hallmark of minor-groove binding without intercalation (*47*). NMR and crystallographic studies of MTA and CRO show hydrophobic contacts in the minor groove, which are fairly conserved among the different analogues (Figure 7). The $\Delta C_p$ values we have derived elsewhere for MTA and MSK (*23*) support the importance of hydrophobic interactions in the entropically driven binding of the aureolic acid antibiotics in the minor groove of DNA. As mentioned above, the binding of other minor groove DNA binders has been fundamentally tested in buffers containing only $Na^+$ ions, and thus, the presence of $Mg^{2+}$ ions complicates the dissection of the various elements that participate in the binding of mithramycins and chromomycins. Divalent counterions act in a complex fashion in the interaction between ligands and DNA, including their direct interaction with the nucleic acid (*44*) and their displacement from DNA upon drug binding (*38*, *39*, *44*). There is an endothermic contribution of the removal of water molecules directly bound to DNA produced by the dehydration effect of $Mg^{2+}$ ions, values that under our experimental conditions, where 1.5 mM $MgCl_2$ was the higher concentration used, are smaller than those reported in the presence of higher concentrations of divalent cations (*16*, *17*, *45*).

A local change from B-DNA to A-DNA has been described as a requirement for the binding of $Mg^{2+}$-coordinated mithramycin dimers to DNA (*2*, *15*). Besides, the A-DNA conformation is considered a dehydrated form of B-DNA (*48*). The titration of DNA with increasing concentrations of $MgCl_2$ indicates that the divalent cation can facilitate such structural transitions in a manner independent of the binding of the $Mg^{2+}$-coordinated antibiotic dimers in the minor groove (Figure 2). Nevertheless, poly(dG)·poly(dC), which displays an A-DNA conformation in the absence of $Mg^{2+}$, does not bind MTA better than other C/G-rich DNAs, while the binding entropy is not markedly different from the values determined for other DNAs (*32*).

Here, we have shown that the formation of $Mg^{2+}$-coordinated antibiotic dimers of a variety of aureolic acid antibiotics takes place at magnesium concentrations lower than those reported elsewhere (*16*, *17*, *32*). Our results are consistent with NMR studies on CRO−DNA complexes showing that the gradual addition of $MgCl_2$ results in a proton spectrum that corresponds to the formation of the DNA−compound complex in slow exchange with the free DNA duplex spectrum, and that the complete switch from the resonances of the free duplex to the DNA−ligand complex occurs upon addition of 1 equiv of $Mg^{2+}$; thus, the complex (containing 2 equiv of the compounds) has the requirement for a single coordinated divalent ion (*15*).

It is worth considering whether the concentrations of magnesium required for forming the $Mg^{2+}$-coordinated antibiotic species that bind to DNA are attainable at the concentrations of $Mg^{2+}$ found in biological fluids and inside cells. Although magnesium concentrations as high as 10 mM have been sometimes regarded as physiological (*17*), such values refer to total magnesium rather than to the free concentrations of intracellular $Mg^{2+}$, the latter constituting less than 5% of the total cell pool [i.e., 95% of $Mg^{2+}$ is bound principally to ATP and proteins (*49*)]. Reports about the concentration of $Mg^{2+}$ in cells are contradictory, and the existing values seem to depend on the technique used for the measurements. The concentration of intracellular free $Mg^{2+}$ in mammalian cells could be between 0.4 and 1.5 mM (*49*, *50*), the latter coinciding with the higher concentrations we have used in our binding experiments. On the other hand, a determination of MTA in plasma and of its elimination half-life, using a radioimmunoassay, indicates the presence of micromolar peak concentrations of this antibiotic (*51*), and thus, $Mg^{2+}$ might be in large excess with respect to the antibiotic. From these considerations, it becomes evident that aureolic acid antibiotics can deal with the concentration of divalent cations that are enough to entail that the species binding in vivo to DNA should be the $Mg^{2+}$-coordinated compound dimers, which may form at magnesium concentrations equivalent to those we have used to examine their binding to DNA (Table 2).

Several aureolic acid antibiotics are very efficient in inhibiting the growth and survival of a variety of human carcinoma cells (*3*, *11*, *19*, *25*, *43*). The cytotoxicity of these molecules can be attributed, at least in part, to their binding to certain gene promoters where they may compete with some transcription factors for their putative binding sites (*18*−*20*, *52*), a property they share with other DNA-binding drugs, which is closely associated with their capacity for binding DNA (see ref *53* and references cited therein). Notably, the new MSK, MSDK, CSK, and CSDK analogues, for which the binding to DNA has been quantified here, exhibit improved antitumor activity and lower toxicity compared to the parental MTA and CRO compounds (*3*, *19*, *21*, *25*).

## ACKNOWLEDGMENT

This work has been conducted within the framework of the 'Xarxa de Referencia en Biotecnologia' of the Generalitat de Catalunya.

## SUPPORTING INFORMATION AVAILABLE

Changes induced by $MgCl_2$ in the visible absorption spectra of mithramycin and chromomycin analogues, optical absorbance spectra of the complexes between DNA and the different analogues in the presence of 200 $\mu$M $MgCl_2$, and changes in the fluorescence spectra of the same analogues in the presence of 200 $\mu$M $MgCl_2$. This material is available free of charge via the Internet at http://pubs.acs.org.

## REFERENCES

1. Lombó, F., Menéndez, N., Salas, J. A., and Méndez, C. (2006) The aureolic acid family of antitumor compounds: Structure, mode of action, biosynthesis, and novel derivatives. *Appl. Microbiol. Biotechnol. 73*, 1–14.
2. Keniry, M. A., Banville, D. L., Simmonds, P. M., and Shafer, R. (1993) Nuclear magnetic resonance comparison of the binding sites of mithramycin and chromomycin on the self-complementary oligonucleotide $d(ACCCGGGT)_2$. Evidence that the saccharide chains have a role in sequence specificity. *J. Mol. Biol. 231*, 753–767.
3. Mansilla, S., Garcia-Ferrer, I., Méndez, C., Salas, J. A., and Portugal, J. (2010) Differential inhibition of restriction enzyme cleavage by chromophore-modified analogues of the antitumour antibiotics mithramycin and chromomycin reveals structure−activity relationships. *Biochem. Pharmacol. 79*, 1418–1427.

4. DeVita, V. T. J., Hellman, S., and Rosenberg, S. A. (2005) Cancer: Principles & Practice of Oncology, 7th ed., Lippincott Williams & Wilkins, Philadelphia.
5. Ogawa, M. (1978) A recent overview of chemotherapy for advanced stomach cancer in Japan. *Antibiot. Chemother. 24*, 149–159.
6. Ferrante, R. J., Ryu, H., Kubilus, J. K., D'Mello, S., Sugars, K. L., Lee, J., Lu, P., Smith, K., Browne, S., Beal, M. F., Kristal, B. S., Stavrovskaya, I. G., Hewett, S., Rubinsztein, D. C., Langley, B., and Ratan, R. R. (2004) Chemotherapy for the brain: The antitumor antibiotic mithramycin prolongs survival in a mouse model of Huntington's disease. *J. Neurosci. 24*, 10335–10342.
7. Jia, Z., Gao, Y., Wang, L., Li, Q., Zhang, J., Le, X., Wei, D., Yao, J. C., Chang, D. Z., Huang, S., and Xie, K. (2010) Combined treatment of pancreatic cancer with mithramycin A and tolfenamic acid promotes Sp1 degradation and synergistic antitumor activity. *Cancer Res. 70*, 1111–1119.
8. Sutphin, P. D., Chan, D. A., Li, J. M., Turcotte, S., Krieg, A. J., and Giaccia, A. J. (2007) Targeting the loss of the von Hippel-Lindau tumor suppressor gene in renal cell carcinoma cells. *Cancer Res. 67*, 5896–5905.
9. Hagiwara, H., Iyo, M., and Hashimoto, K. (2009) Mithramycin protects against dopaminergic neurotoxicity in the mouse brain after administration of methamphetamine. *Brain Res. 1301*, 189–196.
10. Cons, B. M., and Fox, K. R. (1990) Footprinting studies of sequence recognition by mithramycin. *Anti-Cancer Drug Des. 5*, 93–97.
11. Remsing, L. L., González, A. M., Nur-e-Alam, M., Fernández-Lozano, M. J., Braña, A. F., Rix, U., Oliveira, M. A., Méndez, C., Salas, J. A., and Rohr, J. (2003) Mithramycin SK, a novel antitumor drug with improved therapeutic index, mithramycin SA, and demycarosyl-mithramycin SK: Three new products generated in the mithramycin producer *Streptomyces argillaceus* through combinatorial biosynthesis. *J. Am. Chem. Soc. 125*, 5745–5753.
12. Van Dyke, M. W., and Dervan, P. B. (1983) Chromomycin, mithramycin, and olivomycin binding sites on heterogeneous deoxyribonucleic acid. Footprinting with (methidiumpropyl-EDTA)iron(II). *Biochemistry 22*, 2373–2377.
13. Gao, X. L., Mirau, P., and Patel, D. J. (1992) Structure refinement of the chromomycin dimer-DNA oligomer complex in solution. *J. Mol. Biol. 223*, 259–279.
14. Sastry, M., and Patel, D. J. (1993) Solution structure of the mithramycin dimer-DNA complex. *Biochemistry 32*, 6588–6604.
15. Gao, X. L., and Patel, D. J. (1989) Antitumour drug-DNA interactions: NMR studies of echinomycin and chromomycin complexes. *Q. Rev. Biophys. 22*, 93–138.
16. Aich, P., Sen, R., and Dasgupta, D. (1992) Role of magnesium ion in the interaction between chromomycin $A_3$ and DNA: Binding of chromomycin $A_3$-$Mg^{2+}$ complexes with DNA. *Biochemistry 31*, 2988–2997.
17. Aich, P., and Dasgupta, D. (1995) Role of magnesium ion in mithramycin-DNA interaction: Binding of mithramycin-$Mg^{2+}$ complexes with DNA. *Biochemistry 34*, 1376–1385.
18. Jones, D. E., Jr., Cui, D. M., and Miller, D. M. (1995) Expression of $\beta$-galactosidase under the control of the human c-myc promoter in transgenic mice is inhibited by mithramycin. *Oncogene 10*, 2323–2330.
19. Albertini, V., Jain, A., Vignati, S., Napoli, S., Rinaldi, A., Kwee, I., Nur-e-Alam, M., Bergant, J., Bertoni, F., Carbone, G. M., Rohr, J., and Catapano, C. V. (2006) Novel GC-rich DNA-binding compound produced by a genetically engineered mutant of the mithramycin producer *Streptomyces argillaceus* exhibits improved transcriptional repressor activity: Implications for cancer therapy. *Nucleic Acids Res. 34*, 1721–1734.
20. Bataller, M., Méndez, C., Salas, J. A., and Portugal, J. (2008) Mithramycin SK modulates polyploidy and cell death in colon carcinoma cells. *Mol. Cancer Ther. 7*, 2988–2997.
21. Previdi, S., Malek, A., Albertini, V., Riva, C., Capella, C., Broggini, M., Carbone, G. M., Rohr, J., and Catapano, C. V. (2010) Inhibition of Sp1-dependent transcription and antitumor activity of the new aureolic acid analogues mithramycin SDK and SK in human ovarian cancer xenografts. *Gynecol. Oncol. 118*, 182–188.
22. Hou, M. H., Robinson, H., Gao, Y. G., and Wang, A. H. (2004) Crystal structure of the [$Mg^{2+}$-(chromomycin A3)$_2$]-d(TTGGCCAA)$_2$ complex reveals GGCC binding specificity of the drug dimer chelated by a metal ion. *Nucleic Acids Res. 32*, 2214–2222.
23. Barceló, F., Scotta, C., Ortiz-Lombardía, M., Méndez, C., Salas, J. A., and Portugal, J. (2007) Entropically-driven binding of mithramycin in the minor groove of C/G-rich DNA sequences. *Nucleic Acids Res. 35*, 2215–2226.
24. Sastry, M., Fiala, R., and Patel, D. J. (1995) Solution structure of mithramycin dimers bound to partially overlapping sites on DNA. *J. Mol. Biol. 251*, 674–689.
25. Menéndez, N., Nur-e-Alam, M., Braña, A. F., Rohr, J., Salas, J. A., and Méndez, C. (2004) Biosynthesis of the antitumor chromomycin $A_3$ in *Streptomyces griseus*: Analysis of the gene cluster and rational design of novel chromomycin analogs. *Chem. Biol. 11*, 21–32.
26. Rohr, J., Méndez, C., and Salas, J. A. (1999) The biosynthesis of aureolic group antibiotics. *Bioorg. Chem. 27*, 41–54.
27. Blanco, G., Fernández, E., Fernández, M. J., Braña, A. F., Weissbach, U., Kunzel, E., Rohr, J., Méndez, C., and Salas, J. A. (2000) Characterization of two glycosyltransferases involved in early glycosylation steps during biosynthesis of the antitumor polyketide mithramycin by *Streptomyces argillaceus*. *Mol. Gen. Genet. 262*, 991–1000.
28. Rodríguez, D., Quirós, L. M., and Salas, J. A. (2004) MtmMII-mediated C-methylation during biosynthesis of the antitumor drug mithramycin is essential for biological activity and DNA-drug interaction. *J. Biol. Chem. 279*, 8149–8158.
29. Baig, I., Perez, M., Braña, A. F., Gomathinayagam, R., Damodaran, C., Salas, J. A., Méndez, C., and Rohr, J. (2008) Mithramycin analogues generated by combinatorial biosynthesis show improved bioactivity. *J. Nat. Prod. 71*, 199–207.
30. Portugal, J. (2009) Evaluation of molecular descriptors for antitumor drugs with respect to noncovalent binding to DNA and antiproliferative activity. *BMC Pharmacol. 9*, 11.
31. Wang, J. L., and Edelman, G. M. (1971) Fluorescent probes for conformational states of proteins. IV. The pepsinogen-pepsin conversion. *J. Biol. Chem. 246*, 1185–1191.
32. Majee, S., Sen, R., Guha, S., Bhattacharyya, D., and Dasgupta, D. (1997) Differential interactions of the $Mg^{2+}$ complexes of chromomycin $A_3$ and mithramycin with Poly(dG-dC)·Poly(dC-dG) and Poly(dG)·Poly(dC). *Biochemistry 36*, 2291–2299.
33. Pettersen, E. F., Goddard, T. D., Huang, C. C., Couch, G. S., Greenblatt, D. M., Meng, E. C., and Ferrin, T. E. (2004) UCSF Chimera: A visualization system for exploratory research and analysis. *J. Comput. Chem. 25*, 1605–1612.
34. Wang, J., Wolf, R. M., Caldwell, J. W., Kollman, P. A., and Case, D. A. (2004) Development and testing of a general amber force field. *J. Comput. Chem. 25*, 1157–1174.
35. Case, D. A., Darden, T. A., Cheatham, T. E. R., Simmerling, C. L., Wang, J., Duke, R. E., Luo, R., Merz, K. M., Pearlman, D. A., Crowley, M., Walker, R. C., Zhang, W., Wang, B., Hayik, S., Roitberg, A., Seabra, G., Wong, K. F., Paesani, F., Wu, X., Brozell, S., Tsui, V., Gohlke, H., Yang, L., Tang, C., Mongan, J., Hornak, V., Cui, G., Beroza, P., Mathews, D. H., Schafmeister, C., Ross, W. S., and Kollman, P. A. (2006) AMBER, version 9, University of California, San Francisco.
36. Kypr, J., Kejnovska, I., Renciuk, D., and Vorlickova, M. (2009) Circular dichroism and conformational polymorphism of DNA. *Nucleic Acids Res. 37*, 1713–1725.
37. Hou, M. H., and Wang, A. H. (2005) Mithramycin forms a stable dimeric complex by chelating with Fe(II): DNA-interacting characteristics, cellular permeation and cytotoxicity. *Nucleic Acids Res. 33*, 1352–1361.
38. Lohman, T. M. (1986) Kinetics of protein-nucleic acid interactions: Use of salt effects to probe mechanisms of interaction. *CRC Crit. Rev. Biochem. 19*, 191–245.
39. Tan, Z. J., and Chen, S. J. (2006) Nucleic acid helix stability: Effects of salt concentration, cation valence and size, and chain length. *Biophys. J. 90*, 1175–1190.
40. Chaires, J. B. (1997) Possible origin of differences between van't Hoff and calorimetric enthalpy estimates. *Biophys. Chem. 64*, 15–23.
41. Haq, I., Ladbury, J. E., Chowdhry, B. Z., Jenkins, T. C., and Chaires, J. B. (1997) Specific binding of Hoechst 33258 to the d(CGCAAATTTGCG)$_2$ duplex: Calorimetric and spectroscopic studies. *J. Mol. Biol. 271*, 244–257.
42. Remsing, L. L., Bahadori, H. R., Carbone, G. M., McGuffie, E. M., Catapano, C. V., and Rohr, J. (2003) Inhibition of *c-src* transcription by mithramycin: Structure-activity relationships of biosynthetically produced mithramycin analogues using the *c-src* promoter as target. *Biochemistry 42*, 8313–8324.
43. Bataller, M., Méndez, C., Salas, J. A., and Portugal, J. (2010) Cellular response and activation of apoptosis by mithramycin SK in $p21^{WAF1}$-deficient HCT116 human colon carcinoma cells. *Cancer Lett. 292*, 80–90.
44. Marky, L. A., Kupke, D. W., and Kankia, B. I. (2001) Volume changes accompanying interaction of ligands with nucleic acids. *Methods Enzymol. 340*, 149–165.

45. Chakrabarti, S., Mir, M. A., and Dasgupta, D. (2001) Differential interactions of antitumor antibiotics chromomycin $A_3$ and mithramycin with $d(TATGCATA)_2$ in presence of $Mg^{2+}$. *Biopolymers 62*, 131–140.
46. Cons, B. M., and Fox, K. R. (1989) High resolution hydroxyl radical footprinting of the binding of mithramycin and related antibiotics to DNA. *Nucleic Acids Res. 17*, 5447–5459.
47. Chaires, J. B. (2006) A thermodynamic signature for drug-DNA binding mode. *Arch. Biochem. Biophys. 453*, 24–29.
48. Dickerson, R. E. (1992) DNA structure from A to Z. *Methods Enzymol. 211*, 67–111.
49. Maguire, M. E. (1990) Magnesium: A regulated and regulatory cation. In Metal Ions in Biological Systems (Sigel, H., and Sigel, A., Eds.) pp 135−154, Marcel Dekker Inc., New York.
50. Günther, T. (2007) Total and free $Mg^{2+}$ contents in erythrocytes: A simple but still undisclosed cell model. *Magnesium Res. 20*, 161–167.
51. Fang, K., Koller, C. A., Brown, N., Covington, W., Lin, J. R., and Ho, D. H. (1992) Determination of plicamycin in plasma by radioimmunoassay. *Ther. Drug Monit. 14*, 255–260.
52. Wang, L., Guan, X., Zhang, J., Jia, Z., Wei, D., Li, Q., Yao, J., and Xie, K. (2008) Targeted inhibition of Sp1-mediated transcription for antiangiogenic therapy of metastatic human gastric cancer in orthotopic nude mouse models. *Int. J. Oncol. 33*, 161–167.
53. Mansilla, S., and Portugal, J. (2008) Sp1 transcription factor as a target for anthracyclines: Effects on gene transcription. *Biochimie 90*, 976–987.